Neurosci. Bull. January, 2023, 39(1):69–82
https://doi.org/10.1007/s12264-022-00901-1

www.neurosci.cn
www.springer.com/12264

ORIGINAL ARTICLE

Neural Mechanism Underlying Task-Specific Enhancement of Motor Learning by Concurrent Transcranial Direct Current Stimulation

Ying Wang[1,2,3,5] · Jixian Wang[4] · Qing-Fang Zhang[1] · Ke-Wei Xiao[1] · Liang Wang[1] · Qing-Ping Yu[1] · Qing Xie[4] · Mu-Ming Poo[1,2,3,5] · Yunqing Wen[1]

Received: 23 January 2022 / Accepted: 10 April 2022 / Published online: 30 July 2022

Abstract The optimal protocol for neuromodulation by transcranial direct current stimulation (tDCS) remains unclear. Using the rotarod paradigm, we found that mouse motor learning was enhanced by anodal tDCS (3.2 mA/cm^2) during but not before or after the performance of a task. Dual-task experiments showed that motor learning enhancement was specific to the task accompanied by anodal tDCS. Studies using a mouse model of stroke induced by middle cerebral artery occlusion showed that concurrent anodal tDCS restored motor learning capability in a task-specific manner. Transcranial *in vivo* Ca^{2+} imaging further showed that anodal tDCS elevated and cathodal tDCS suppressed neuronal activity in the primary motor cortex (M1). Anodal tDCS specifically promoted the activity of task-related M1 neurons during task performance, suggesting that elevated Hebbian synaptic potentiation in task-activated circuits accounts for the motor learning enhancement. Thus, application of tDCS concurrent with the targeted behavioral dysfunction could be an effective approach to treating brain disorders.

Keywords Motor learning · tDCS effect · Neural mechanism of tDCS · Neuronal excitability · Stroke model mouse

Ying Wang and Jixian Wang contributed equally to this work.

Supplementary Information The online version contains supplementary material available at https://doi.org/10.1007/s12264-022-00901-1.

✉ Mu-Ming Poo
mpoo@ion.ac.cn

✉ Yunqing Wen
wenyq@ion.ac.cn

1 Institute of Neuroscience, State Key Laboratory of Neuroscience, Key Laboratory of Primate Neurobiology, Center for Excellence in Brain Science and Intelligence Technology, Chinese Academy of Sciences, Shanghai 200031, China

2 University of Chinese Academy of Sciences, Beijing 100049, China

3 School of Life Science and Technology, ShanghaiTech University, Shanghai 201210, China

4 Department of Rehabilitation Medicine, Ruijin Hospital, Shanghai Jiao Tong University School of Medicine, Shanghai 200025, China

5 Shanghai Center for Brain Science and Brain-Inspired Intelligence Technology, Lingang Laboratory, Shanghai 201210, China

Introduction

Transcranial direct current stimulation (tDCS) is now widely used for non-invasive modulation of brain functions in healthy subjects and patients with brain disorders, ranging from neurological and psychiatric diseases to stroke-induced dysfunction [1–4]. For example, many previous reports have demonstrated that tDCS applied to the primary motor cortex (M1) improves motor function in stroke patients [5, 6], but other studies have yielded no significant effects [7]. Neuromodulation by tDCS has also been used to alleviate cognitive deficits, such as in working memory [8–10], attention [11–13], and the expression and comprehension of language [14–16], with both positive and negative results. The variability of tDCS effects could be attributed to the large variation in the stimulus parameters (current intensity, duration, timing, polarity, and stimulation site), electrode configurations, and individual differences among patients. To define the optimal treatment parameters and protocols, understanding the neural mechanisms underlying the action of tDCS on

the brain is critical. Furthermore, the effects of an individual patient's cranial anatomy on the pattern of current distribution within the brain needs to be considered.

Another important parameter is the timing of tDCS application relative to the patient's performance of the targeted behavior. In treating the motor deficits of stroke patients, anodal [5, 6] or cathodal [5] tDCS has been found to produce positive effects on motor function. Some studies have also shown that tDCS combined with the targeted motor task improves motor function [17, 18]. However, a meta-analysis has shown no conclusive advantage of coupling tDCS with cognitive training as compared to tDCS alone [19]. In this study, we specifically compared the effects of tDCS on motor learning between tDCS that was applied during ("online") and before or after ("offline") the motor task training in mice. We found strong evidence that only online anodal tDCS could enhance motor learning, and the effect was task-specific.

Computational modeling studies have predicted the direction and distribution of electrical fields in the human brain produced by tDCS, demonstrating that current flows predominantly parallel to the cortical surface [20, 21]. The modeling results also suggest that axon terminals are more susceptible to current-induced polarization than the soma [20]. Measurements of motor evoked potentials elicited by transcranial magnetic stimulation (TMS) indicated that anodal tDCS of the human motor cortex for 9–13 min induced sustained elevation of cortical excitability [22], whereas cathodal tDCS for 9 min caused prolonged inhibition of cortical excitability [23]. Direct current stimulation (DCS) of mouse brain slices has shown that DCS combined with low-frequency synaptic activation induces long-lasting synaptic potentiation, an effect that is dependent on N-methyl-D-aspartate receptor activation and brain-derived neurotrophic factor [24]. Using *in vivo* two-photon Ca^{2+} imaging to directly monitor cortical activity in the primary visual cortex of urethane-anaesthetized mice, Monai *et al.* [25] found that tDCS activates Ca^{2+} elevation in astrocytes but not in neurons. The mechanism underlying the cell-type specificity in the latter study remains unclear. It may be caused by higher expression of the Ca^{2+}-sensor in astrocytes [26] or the anaesthetized state of the animal. In the present study, we applied *in vivo* transcranial two-photon Ca^{2+} imaging through the thinned skull to examine neuronal activity in the relatively intact M1 of awake mice, particularly the effects of anodal and cathodal tDCS on the activity of M1 neurons related and unrelated to a motor task. Our results largely confirm the excitatory and inhibitory effects on cortical neurons predicted by computational modeling, and provide a direct mechanistic interpretation of the task-specific effects of tDCS on motor learning.

In the present study, we specifically tested the hypothesis that modulation of neuronal spiking due to tDCS-induced membrane potential changes [27–29] is effective in modulating those neural circuits that are active at the time of tDCS [2, 29]. Using rotarod-running and beam-walking paradigms, we assessed the enhancing effect and task specificity of online and offline tDCS on motor learning. In both normal wild-type mice and a mouse model of stroke, we found that applying anodal but not cathodal tDCS to M1 during task training markedly enhanced motor learning in a task-specific manner. Together, our findings showed that the concurrent application of anodal tDCS with motor task training is effective in promoting motor learning, and provide a mechanistic interpretation of this effect based on cortical neuronal excitation.

Materials and Methods

Mice

The primary objective of this study was to investigate the neural mechanism underlying the modulation of motor learning by tDCS. All animal procedures were approved by the Animal Committee of the Institute of Neuroscience (ION)/Center for Excellence in Brain Science and Intelligence Technology, Chinese Academy of Sciences. In behavioral experiments, male wild-type C57BL/6J mice (7–10 weeks old, from Shanghai Slac Laboratory Animal Co., Ltd, China) were randomly assigned to two groups in each experiment: tDCS-treated and sham (no current)-treated. Male wild-type C57BL/6J mice (8–14 weeks old from Slac Co.) with middle cerebral artery occlusion (MCAO) were used. For *in vivo* two-photon imaging of neuronal activity, transgenic mice expressing Thy-1 GCaMP6s (8–14 weeks old, male/female, background strain C57BL/6, from the Jackson Laboratory, Bar Harbor, USA) were used. The numbers of mice in each experiment are described in the figure legends and main text. Mice were housed under a 12-h light-dark cycle (lights on from 07:00 to 19:00) at room temperature (19–22°C) in the ION animal facility. Efforts were made to limit the number of animals used and to minimize their suffering. Each set of behavioral experiments was conducted during a fixed period each day. Two-photon experiments were performed either during daytime or at night, depending on the availability of the equipment.

Electrode Implantation for tDCS

We adopted a unilateral epicranial electrode configuration that was previously used for tDCS in rodents [30]. The stimulating electrode consisted of an epicranial implanted tubular plastic jack (inner area 3.14 mm^2) for behavioral experiments and a circular wire surrounding the chamber above the observation window (area ~3 mm^2) for imaging experiments; the jack and chamber were filled with saline (0.9% NaCl) prior

to stimulation. The reference electrode was a round tin plate (~5 mm in diameter) implanted under the contralateral skin on the back of the neck. For electrode implantation, mice were anesthetized by intraperitoneal (i.p.) injection of pentobarbital sodium (7 mg/kg) and positioned in a stereotaxic frame (model 68030, RWD Life Science Co., Ltd, Guangdong, China), the scalp and underlying tissue were removed, and the center of the active electrode was positioned unilaterally on the skull over M1 at the stereotaxic coordinates: 0 mm posterior from bregma and 1.5 mm lateral from the midline. During surgery, the body temperature was maintained at 38°C with a heating pad. All mice were allowed to recover for 7 days before experiments. tDCS (current: 0.05, 0.1, and 0.2 mA in behavioral experiments; 25 and 50 μA in imaging experiments) was delivered to the right M1 with a stimulator (model ST1, Quanlan Technology Co., Ltd, Shanghai, China). For online tDCS on mice performing the beam-walking task, custom-made wireless stimulators were used.

Training on the Rotarod Running Task

Mice were familiarized with the experiment room for 2 h. A 5-lane rotarod (3 cm in diameter, model 47600, Ugo Basile Inc., Gemonio, Italy) was used to assess motor skill acquisition in tDCS-treated and sham-treated mice. Prior to the training period each day, each mouse was given a 5-min familiarization period on the rotarod at a constant low rotation speed (days 1 and 2, 4 r/min; days 3 and 4, 8 r/min). At the same time of day on each of four consecutive training days, the mice were trained in three 5-min rotarod running trials (days 1 and 2, 4–40 r/min; days 3 and 4, 8–80 r/min) [31], interleaved with 5-min rest periods off the rotarod. This procedure was a sensitive assay for assessing motor learning, because the performance of some mice on the easier rotarod (at 4–40 r/min) reached a ceiling at 40 r/min within 2 days, and doubling the rotation speed allowed mice to show a greater degree of motor learning in the following days. We found that this procedure produced consistent motor learning behavior among different groups of mice and under several different test conditions, such as dual motor tasks. Each trial ended when a mouse fell off the rotarod or turned one full revolution, or had reached a duration of 300 s on the rotarod [32]. "Online" tDCS was applied during each trial, and the current stimulation was absent during inter-trial intervals (ITIs). "Offline" tDCS was applied when the animals were not performing the task. Digital video was recorded during the training for later analysis.

Dual-task Training for Rotarod Running and Beam Walking

After the training for rotarod running each day as described above, the mice were allowed to rest for ~5 h in their home cages before training for the beam-walking task. The beam-walking training followed that described previously [33], consisting of walking across a 100 cm-long beam with 25-, 7-, or 3-mm wide. Light onset at the start point in the dark room triggered the mouse to walk towards the dark chamber at the other end of the beam. The mice were trained over four consecutive days. Each day, a mouse was familiarized on the 25 mm-wide beam, followed by 3 training trials (days 1 and 2, 7-mm beam; days 3 and 4, 3-mm beam). Mice had a 2-min ITI rest in their home cages. A soft cloth was stretched below the beam to protect mice in case of a fall. A video camera was placed on each side of the beam to record the crossing time and the number of hindlimb slips over a standard 80-cm length of the beam. Slips of both hindlimbs were counted for normal mice, and only slips of the hindlimb contralateral to the lesioned cortex were counted for MCAO mice.

Transcranial *in vivo* Two-Photon Imaging

For two-photon imaging, surgery was performed with mice under anesthesia with an 1%–1.5% isoflurane and oxygen mixture, during which the body temperature was maintained at 38°C with a heating pad. After exposure of the skull, a metal frame was attached to the skull with dental acrylic, and the skull was thinned over a circular region (~2 mm in diameter) above M1 (window center: bregma, 0 mm; mediolateral, 1.5 mm), first with a high-speed micro-drill, then by thinning of the inner compact bone layer with a microsurgical blade until blood vessels became clearly visible under the skull. Final skull thickness estimated by post-thinning histological measurements was 15.9 ± 0.86 μm ($n = 4$ mice).

For two-photon imaging, mice were first trained for 1 day on the rotarod, and images were then acquired on a treadmill rotating at 23.6 mm/s (equivalent to a rotarod rotation speed of 15 r/min), and the animal's behavior was monitored by an infrared camera. Two-photon imaging was applied with a resonant scanner-based B-Scope (Thorlabs Inc., Newton, NJ, USA), at an excitation wavelength of 910 nm (Ti-Sa laser, Spectra-Physics, Milpitas, CA, USA) and a field-of-view (FOV) of 350×350 μm^2 (512×512 pixels) under a 16× objective (NA 0.8; Nikon Instruments Inc., Tokyo, Japan). Images were acquired using ThorImage software at a frame rate of 15.6 Hz for 25 or 30 min depending on the experimental goal. Mice were trained in two behavioral paradigms with tDCS. In the first paradigm (Fig. 3), mice were run on the treadmill at a constant speed ("task" state) or rested on the treadmill ("rest" state). Measurements of Ca^{2+} signals included 5 min at baseline before and after two 5-min tDCS sessions, which were also separated by 5-min baseline (total imaging time 25 min). In the second paradigm (Fig. 4), in the task state, mice began running on the treadmill following 5-min rest on the treadmill, and 5-min tDCS was applied to M1 after running for 10 min on the treadmill, followed by 10

min running (total running time 25 min, total imaging time 30 min). In the rest state, 5-min tDCS was applied 5 min after the onset of the experiment on the treadmill, followed by 10 min rest (total imaging time 20 min).

MCAO

Rodent models of focal cerebral ischemia have been developed to mimic human ischemic stroke, using the procedure of intraluminal suture occlusion of the middle cerebral artery [34]. This MCAO mouse model has been widely used to study stroke-induced pathophysiology such as cell death and changes in synaptic structures [35–37], and to design new prophylactic, neuroprotective, and therapeutic agents [38]. The mice were anesthetized with pentobarbital sodium (7 mg/kg, i.p.) and body temperature was maintained at 38 °C during surgery. A midline incision was made at the neck and the left common carotid artery (CCA), external carotid artery (ECA), and internal carotid artery (ICA) were identified and ligated. For MCAO, a silicone-coated round-tipped MCAO suture (MSMC21B120PK50, RWD Life Science Co.) was gently inserted from the ECA stump to the ICA, up to ~10 mm, stopping at the MCA, following the previously reported method [39]. After 90, 60, or 0 min of occlusion, the MCAO suture and ligation were withdrawn. The neck skin was sewn back after blood reperfusion was confirmed.

TTC (2,3,5-Triphenyltetrazolium Chloride) Staining and Laser Speckle Contrast Imaging (LSCI)

One day after reperfusion, mice were anesthetized with pentobarbital sodium (7 mg/kg, i.p.), and their brains were removed for histology. A series of 2-mm coronal slices were cut (model 68707, RWD Life Science Co.). The infarct area was shown using the TTC (2%, Sigma, Darmstadt, Germany) staining method as described previously [40]. In the imaging procedure, the mice were anesthetized with pentobarbital sodium (7 mg/kg, i.p.) and a midline incision was made to expose the skull for LSCI before, during, and after MCAO, following the previously reported method [41]. The LSCI images before MCAO were used as baseline images. The exposure time for each image was 5 msec and the frame rate was 50.6 frames per second. In the LSCI system (RFLSI III, RWD Life Science Co.), the cortex was illuminated by a reshaped laser beam from a 785-nm laser diode. Two hundred speckle images were recorded in each imaging section.

Quantification in Two-Photon Imaging

In two-photon imaging, the fluorescence signals were quantified using Matlab-based software (The Mathworks Inc., Natick, MA, USA) after movement correction of the image stacks with a Turboreg plugin (ImageJ, National Institutes of Health) [42]. The fluorescence of single cells was measured over the region covering each neuronal soma, which was defined by the image stack. The fluorescence change $\Delta F/F_0$ was defined as $(F–F_0)/F_0$, where F_0 is the baseline fluorescence averaged over a 5-min period before the onset of the first tDCS. To summarize the data from all mice, we calculated the average $\Delta F/F_0$ during the last 2 min of tDCS by the average values during the 2-min baseline period prior to tDCS for each mouse. To analyze the persistent alteration of activity post-tDCS, we measured the average fluorescence changes ($\Delta F/F_0$) during the last 30 s of every tDCS period and during the subsequent post-tDCS activity in 30-s bins for 5 min.

Statistics

For behavioral training, rotarod data for "time on rod" and "terminal speed", and beam-walking data for "number of slips" were analyzed by two-way ANOVA. Data for learning rates on the rotarod and beam walking were analyzed using the two-tailed unpaired *t*-test. For two-photon imaging data, significance tests were applied between data obtained during anodal/cathodal tDCS and baseline (2 min before each tDCS onset) using the two-tailed paired t-test. The statistical analyses were calculated using GraphPad Prism (Version 5.0, GraphPad, San Diego, CA, USA). Data were considered significantly different if $*P < 0.05$ or $**P < 0.01$.

Results

Online Anodal tDCS Enhances Learning of the Rotarod Running Task in Mice

Mice were subjected to a rotarod running task that began each day with a 5-min familiarization period at a constant low rotation speed, followed by three 5-min trials with gradually increasing speed [31] that were spaced with 5-min ITIs off the rotarod (Fig. 1A). Mice received tDCS at designated times with anodal ("+") or cathodal ("–") currents, or without current (sham control, "S") (Fig. 1B). The mouse normally learned the task well over four training days, as shown by the increasing duration of staying on the rotarod (Fig. 1C) and increasing terminal rotor speed when the mouse fell off the rotarod (Fig. 1D). When tDCS was applied to the right M1 during the familiarization period and all three task trials each day ("online" stimulation), we found a significant increase in both the time on the rotarod and the terminal speed, beginning on the second day of training (Fig. 1C, Online, $n = 13$ mice; Sham, $n = 10$ mice, and movies S1, S2). This enhancement of motor learning was still detectable on day 14 but not day 28 after training (Fig. S1, A, B; same n as above). The results were further quantified by the

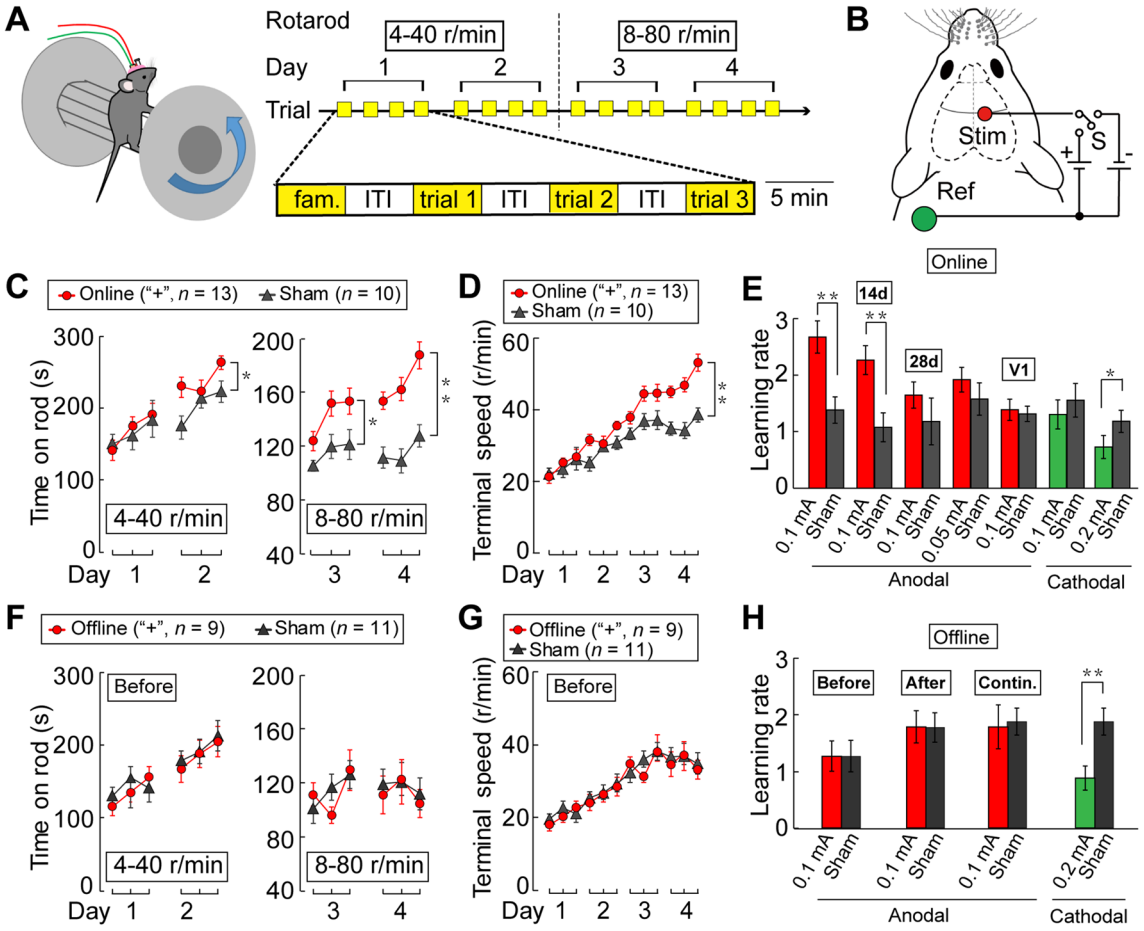

Fig. 1 Effects of tDCS on mouse learning of the rotarod running task. **A** Training protocol. Each day, the mouse performs a 5-min familiarization trial (fam) at a constant low speed, followed by three 5-min trials [separated by 5 min inter-trial intervals (ITI)] at a linearly-increasing rotation speed (days 1 and 2, 4–40 r/min; days 3 and 4, 8–80 r/min). **B** Schematic of the electrode configuration [Stim, tDCS electrode; Ref, reference electrode; S, sham (no current); +, anodal; –, cathodal]. **C** Average time on the rotarod during each trial. **D** Terminal rotation speed at which mice fall off the rotarod during each trial. Online, anodal tDCS (0.1 mA) is applied during each trial; *n*, total number of mice. **E** Summary of results showing the learning rate, as defined by the normalized difference of terminal speed between the last and the first trials of the entire training period. Data depict standard 4-day training with (colored bars) and without (sham, black bars) online anodal or cathodal tDCS applied to M1 at different current amplitudes (14d and 28d, results obtained with 3 additional training trials at 14 and 28 days after training. V1, tDCS applied to primary visual cortex instead of M1). **F–H** As for **C–E**, but tDCS is applied during ITIs. Before and After, average values with tDCS applied during ITIs before and after each trial; Contin., 20-min continuous tDCS applied before the familiarization trial. Error bars, SEM; $^*P < 0.05$, $^{**}P < 0.01$, two-way ANOVA in **C, D, F, G**; unpaired *t* test in **E, H**.

rate of learning, as defined by the normalized difference of the terminal speed between the first and last training trials (Fig. 1E; same *n* as above). Doubling the anodal tDCS current to 0.2 mA caused occasional convulsions, and reducing the current to 0.05 mA resulted in no learning enhancement (Figs 1E and S2A, B; $n = 11$ for both Online and Sham). We thus chose 0.1 mA for the standard anodal tDCS in this study. Furthermore, we found no enhancement of rotarod learning when the same online anodal tDCS was applied to the primary visual cortex Fig. 1E and Fig. S3A, B; Online, $n = 11$; Sham, $n = 12$), indicating a stimulation site-specific tDCS effect. The rotarod learning was not affected by the surgical procedure and electrode installation, as shown by comparison of the motor learning in mice that were not subjected to the procedure (Fig. S4A, B; Surgery, $n = 9$; Control, $n = 12$).

In contrast to the learning enhancement described above, we found that anodal tDCS (at 0.1 mA) applied during all 5-min ITIs before or after rotarod running ("offline" stimulation) had no effect on the rate of rotarod learning (Figs 1F–H and S5A, B; "After": Offline, $n = 12$, Sham: $n = 11$). Furthermore, no effect was found when anodal tDCS was applied continuously for 20 min before the task onset (Figs 1H and S5C, D; "Contin.": Offline: $n = 12$, Sham: $n = 11$), a protocol often used in clinical research [43]. In contrast to anodal tDCS, online *cathodal* tDCS (0.1 mA) at M1 also had

no effect on rotarod learning (Figs 1E and S6A, B; Online: $n = 7$, Sham: $n = 5$). However, when the cathodal current was increased to 0.2 mA, learning was impaired on days 3 and 4 of training (Figs 1E and S6C, D; Online: $n = 8$, Online sham: $n = 8$). Unlike that found for anodal tDCS, both online and offline cathodal stimulation at 0.2 mA resulted in similar impairment of learning (Figs 1E, H and S6C, D). As shown later, this may be attributed to the long-lasting (>5 min) suppression of neuronal firing by cathodal tDCS. Taken together, these findings showed that tDCS bi-directionally modulates rotarod learning, and that the enhancing effect is significant only when anodal tDCS is applied concurrently with the performance of the rotarod task.

Task-specific Enhancement of Motor Learning by Anodal tDCS

The effect of online anodal tDCS on motor learning may be attributed to the specific enhancement of rotarod-running skill or improvement of motor coordination in general. To address this issue, we introduced a beam-walking learning task, in which the mouse was given a short familiarization period for walking along a wide beam (25 mm wide), followed by 3 trials of walking on a narrow beam each day (days 1 and 2, 7 mm; days 3 and 4, 3 mm; Fig. 2A). The learning process was shown by a gradual reduction in the mean number of hindlimb slips and the mean traverse time during beam walking, and the learning rate was quantified by the normalized difference in the mean number of slips between the last and the first beam-walking trial on the 3-mm beam over the 4-day training period.

In the first set of experiments, we measured beam walking before and after 4 days of rotarod training, and the former was not affected by the latter, as reflected by a reduction of hindlimb slips similar to that in untrained mice (Fig. S7A–C; Rotarod: $n = 10$, Control: $n = 12$). This implied that motor learning was specific to the trained motor task. In the second set of experiments, we trained the mice to perform both rotarod running and beam walking (dual tasks) each day over four training days, and found that rotarod learning did not affect the learning rate for beam walking, which was comparable to that resulting from beam-walking training alone (Fig. S8A–C; Rotarod: $n = 10$, Control: $n = 12$). Thus, there was no transfer of learning from rotarod running to beam walking. Importantly, when we enhanced the rotarod learning with online anodal tDCS, the learning rate for beam walking was not affected in the dual-task training (Fig. 2B–D; Online: $n = 11$, Sham: $n = 12$). Conversely, when the learning of beam walking was enhanced by online anodal tDCS (Fig. S9A, B and movies S3–6; Online: $n = 15$, Sham: $n = 15$), we found no enhancement of learning for rotarod running (Fig. S10A–D; Online: $n = 18$, Sham: $n = 17$). Thus, online anodal tDCS during a specific task did not lead to general enhancement of motor learning. In contrast to this specific anodal tDCS effect, we found that both online and offline *cathodal* tDCS during rotarod training had suppressive effects on learning both rotarod running (Fig. 2E, G; Online: $n = 11$, Offline: $n = 12$, Sham: $n = 12$) and beam walking (Fig. 2F, G; Online: $n = 11$, Offline: $n = 12$, Sham: $n = 12$).

Modulation of Neuronal Activity by Anodal and Cathodal tDCS

We next investigated the action of tDCS on the activity of M1 neurons using transcranial *in vivo* two-photon Ca^{2+} imaging. We used *thy-1* transgenic mice expressing the Ca^{2+}-sensitive fluorescent protein GCaMP6s in cortical neurons, and monitored the spiking activity of individual neurons by measuring the elevation of GCaMP6s fluorescence [44] through the skull after a skull-thinning procedure. The activity of cortical neuron populations in layers II/III of M1 was recorded in head-fixed mice on a treadmill that alternated between "task" (during running on the steadily moving treadmill at 23.6 mm/s) and "rest" (during resting on the stationary treadmill, at zero velocity) states (Fig. 3A). We recorded substantial spontaneous activity in M1 neurons, as reflected by pulsatile changes in the fluorescence signal (Fig. 3B, movie S7), which is known to correlate with the spiking rates of neurons [44, 45]. When anodal tDCS was applied through a saline pool above the thinned skull, we recorded a gradual increase in the fluorescence signals in many neurons (movie S7). Figure 3C ($n = 6$ cells) illustrates the fluorescence changes ($\Delta F/F_0$) in 6 example neurons (boxed in Fig. 3B) during the task and rest periods when two consecutive anodal or cathodal tDCS were applied (each for 5 min). An apparent elevation of Ca^{2+} activity by anodal tDCS (25 μA) occurred in 4/6 neurons during the task but not the rest period, and all 6 neurons showed strong inhibition of activity during cathodal tDCS (50 μA) (Fig. 3C). The same group of cells were monitored before and after two episodes of anodal and cathodal tDCS sequentially under the task and rest conditions.

The reproducibility of the effects of tDCS on neuronal activity was examined in separate experiments on 8 mice where either anodal or cathodal tDCS was repeated after an interval of 5 min (Fig. 3D). Significant elevation of fluorescence signals was induced by anodal and suppression by cathodal tDCS during the task period (Fig. 3E, F; $n = 8$ mice). We also noted that changes in the average fluorescence subsided gradually after each tDCS offset, and that the suppressive effect of cathodal tDCS persisted for longer than the enhancement effect of anodal tDCS (Fig. 3G; $n = 8$ mice). This may account for the offline suppressive effect on the rotarod learning described above using only 5-min ITIs in the present paradigm.

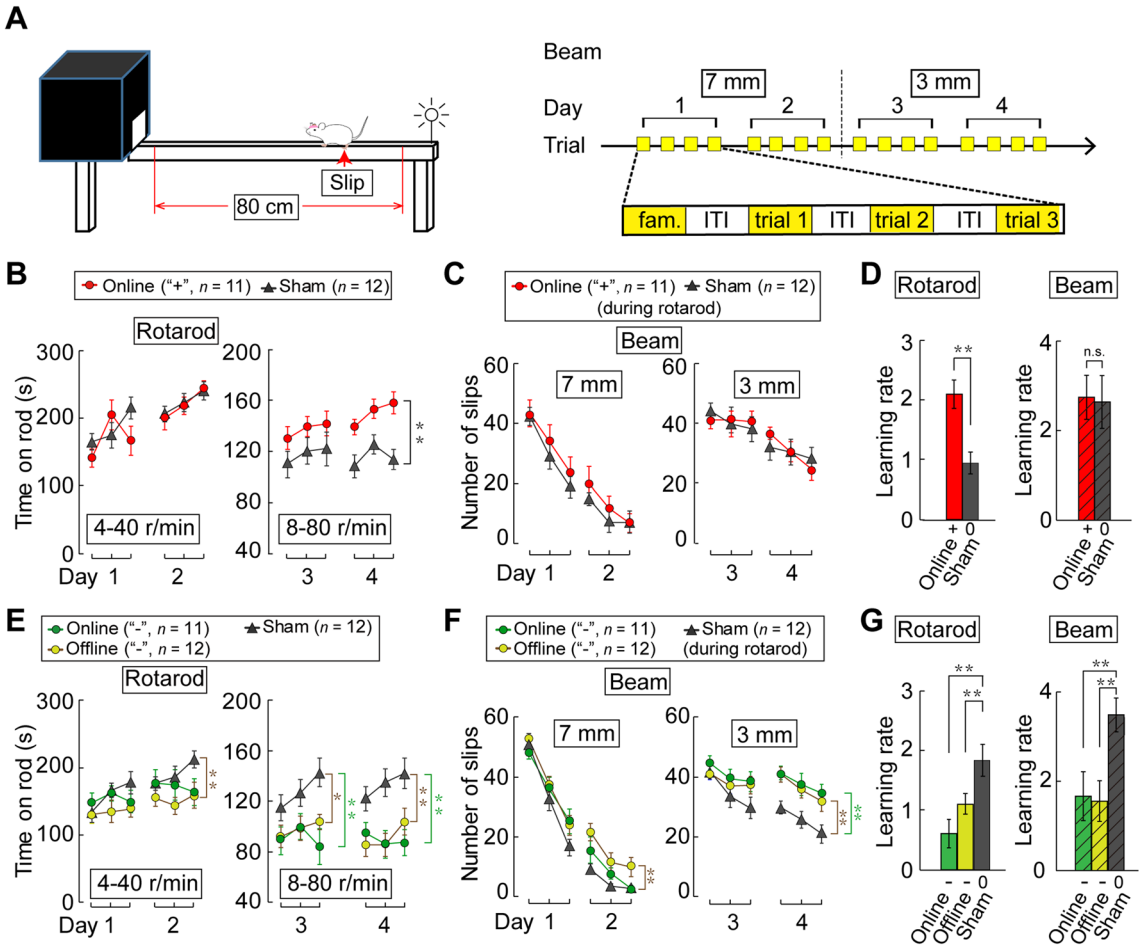

Fig. 2 Effects of tDCS-induced modulation of rotarod learning on the learning of beam walking. **A** Experimental protocol of beam walking. The mouse is subjected to anodal online tDCS as in Fig. 1C, except that the rotarod task is followed by a beam walking learning task in the absence of tDCS. Each mouse is familiarized to a wide beam (25 mm), followed by three trials on a thinner beam (days 1 and 2, 7 mm; days 3 and 4, 3 mm). **B**, **C** Data from dual-task experiments. **B** Average time on the rotarod is presented as in Fig.1C. **C** The average frequency of hindlimb slips is reduced during the 4-day training for beam walking. Note that online anodal tDCS during rotarod running improves rotarod learning (**B**), but has no effect on learning beam walking (**C**). *n*, total number of mice. **D** Summary of results showing learning rates for the rotarod and beam walking, as defined by normalized difference of the slip frequencies between the last and the first trials of walking on the 3-mm beam. **E–G** Learning the rotarod and beam walking with cathodal online (or offline) tDCS during rotarod learning. +, anodal tDCS; –, cathodal tDCS; 0, no current. Error bars, SEM; $*P < 0.05$, $**P < 0.01$, two-way ANOVA in **B, C, E, F**; unpaired *t* test in **D, G**.

The M1 neurons monitored in the above experiments may have included neurons that were activated to perform the treadmill-running task and those unrelated to the task. We thus further inquired whether the tDCS effects differed between these two types of neuron. The activity of all GCaMP6s-expressing M1 cells within the field of view were monitored for 5 min before the task onset to obtain a baseline (Fig. 4A). Task-related and un-related cells were defined by their peak fluorescent signal ($\Delta F/F_0$) within the first 2-min window after the task onset that were above the level of baseline + 1.5 SD and below the level of baseline + 0.5 SD, respectively. Data from all task-related cells ("+", $n = 247$ cells; "–", $n = 158$ cells) and task-unrelated cells ("+", $n = 22$ cells; "-", $n = 54$ cells) identified in 4 mice were summarized by activity heatmaps and average activity profiles (Fig. 4A). We found that, during the task period, anodal tDCS induced a highly significant elevation of activity in task-related cells, but not in task-unrelated cells. By contrast, the same anodal tDCS of this population of neurons during the rest period had no significant effect on either type of cell (Fig. 4A, B). The inhibitory effect of cathodal tDCS, however, was strongly pronounced during both task and rest periods in all neurons (Fig. 4A, B). These results support the notion that the specific effect of anodal tDCS on motor learning is due to elevation of the activity of task-related neuronal circuits.

Taken together, these results support the hypothesis that anodal and cathodal tDCS modulate neuronal firing by

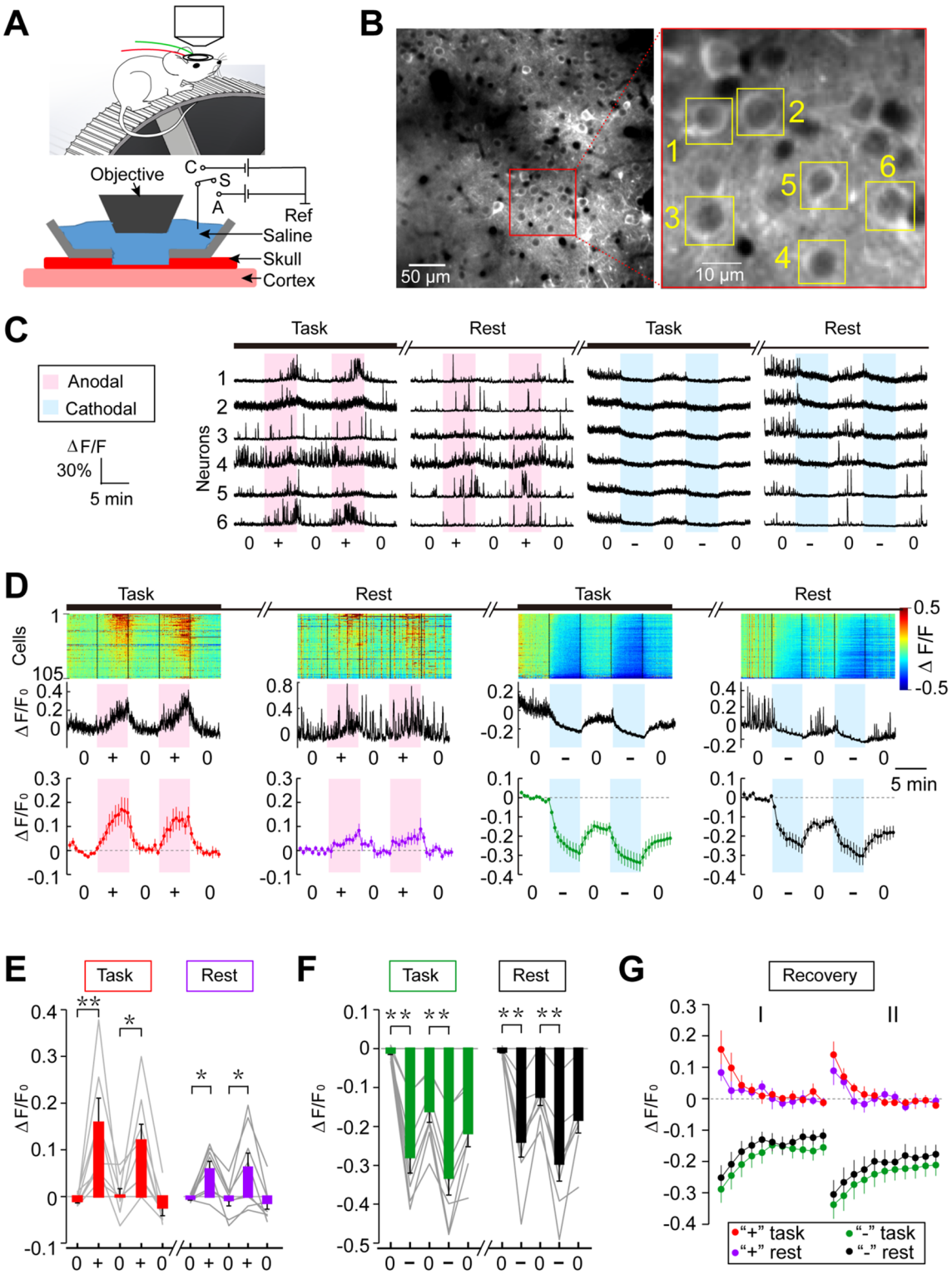

inducing depolarization and hyperpolarization of cortical neurons, respectively, consistent with previous findings on isolated brain slices [24, 46, 47]. When applied at the time of specific motor circuit activation, as during a motor task, anodal tDCS facilitates the learning-associated modification of specific motor circuits in M1 *via* enhancing correlated firing that induces Hebbian long-term potentiation of synapses within these circuits.

◂**Fig. 3** Transcranial two-photon imaging of tDCS-induced modulation of cortical neuronal activity. **A** Schematic depicting the optical window over the thinned skull for two-photon imaging of M1 neurons in a head-fixed mouse on a treadmill that moves at a constant speed during the task. **B** Example images of Thy1-GCaMP6s-expressing neurons in M1, viewed through the imaging window. Red-boxed region is shown at higher resolution on the right, revealing GCaMP6s fluorescence of individual layer II/III neurons. **C** Changes of GCaMP6s fluorescence ($\Delta F/F_0$) with time monitored in six M1 neurons (marked by boxes in **B**). Pink, duration of anodal tDCS at 25 μA; blue, duration of cathodal tDCS at 50 μA. **D** Fluorescence changes of all labelled cells within the image field, recorded from one mouse. Upper panel, amplitude of $\Delta F/F_0$ for each cell with time is color-coded (scale on right). The cells are ordered according to the peak values of $\Delta F/F_0$. Middle panel, average $\Delta F/F_0$ for all cells shown above, Lower panel, average $\Delta F/F_0$ for all cells from 8 mice. **E**, **F** Summary of tDCS-induced GCaMP6s fluorescence changes for data from all mice ($n = 8$). Average fluorescence changes ($\Delta F/F_0$) during the last 2-min of tDCS are normalized by the average values during the 2-min baseline period prior to tDCS, for two consecutive trials under task and rest conditions. Data for the same set of neurons in each mouse are connected by lines ($^*P < 0.05$, $^{**}P < 0.01$, paired *t* test). **G** Post-treatment persistence of tDCS effects shown by the average fluorescence changes with time, normalized by the values at the time of termination of anodal or cathodal tDCS, for task and rest conditions. Error bars, SEM.

Task-Specific Restoration of Motor Learning by tDCS in a Mouse Model of Stroke

Meta-analyses have shown high variability in the clinical efficacy of tDCS for treating stroke patients [48, 49]. This variability could be attributed in part to differences in the tDCS protocol and individual stroke conditions. In this study, we examined the effect of tDCS on motor learning in a relatively well-defined mouse model of stroke. Standard MCAO for 60 or 90 min induced a large left hemisphere lesion within the left somatosensory cortex and part of the motor cortex at day 1 after MCAO (Fig. 5A). When these mice were subjected to rotarod learning at 14 days after MCAO (Fig. 5A), we found their motor coordination was significantly impaired, as shown by an overall reduction in the time on the rotarod and the rate of rotarod learning, compared to control mice that underwent MCAO surgery without sustained artery occlusion (Fig. 5B, C; MCAO: $n = 11$ mice, Control: $n = 12$ mice). Furthermore, online anodal tDCS at the left perilesional M1 region (Fig. 5A) largely restored the learning of motor coordination and rotarod running (Fig. 5B, C, E; and movie S9, 10; MCAO: $n = 11$, MCAO/Online: $n = 11$). In contrast, offline *anodal* tDCS (Figs 5F and S11A, B; MCAO/Offline, $n = 11$, MCAO, $n = 11$), online *cathodal* tDCS (Fig. S12A; MCAO/Online, $n = 8$; MCAO, $n = 9$), and offline *cathodal* tDCS (Fig. S12B; MCAO/Offline, $n = 7$; MCAO, $n = 9$) at the same site all had no effect on learning motor coordination and rotarod running in MCAO mice.

In the absence of tDCS, 90-min MCAO impaired motor learning of both rotarod running and beam walking, compared to control mice (Fig. 5B–E; MCAO: $n = 11$; Control, $n = 12$). However, the mice that had rotarod learning restored by online anodal tDCS did not show improved learning of beam walking, as compared to those subjected to sham tDCS during rotarod running (Fig. 5B–E; MCAO: $n = 11$, MCAO/Online: $n = 11$). In contrast, offline anodal tDCS during rotarod training had no effect on learning either rotarod running or beam walking (Figs 5F and S13A–D; MCAO: $n = 12$, MCAO/Offline: $n = 14$). Therefore, the restoration of rotarod learning in MCAO mice by anodal tDCS was task-specific, rather than a general restoration of motor learning. Based on the above finding of elevated neuronal firing induced by anodal tDCS, the restoration of rotarod learning may involve the specific enhancement of residual neural circuits after MCAO that were activated during rotarod running, without affecting those underlying beam walking.

Discussion

The timing of tDCS relative to targeted task performance has been addressed in previous studies of healthy human subjects and stroke patients, but conflicting results have been reported, as summarized by meta-analyses [48, 49]. For example, online but not offline anodal tDCS of M1 during a motor sequence task has been found to enhance motor learning, while online cathodal tDCS has no or opposite effects [50, 51]. However, another study using offline anodal tDCS prior to the motor task in human subjects showed an enhancing effect on motor learning [52]. In cases of prolonged tDCS, the effects on the human motor cortex can last for hours [22] and even days [53], so the timing of tDCS becomes less relevant. A previous study using mouse brain slices showed that only DCS coupled with low-frequency synaptic activation can induce long-lasting synaptic potentiation [24]. Direct current stimulation time-locked to the expected onset of low-frequency oscillations (< 4 Hz) also significantly improves skilled reaching in stroke model rats [54]. Our present results further underscore the importance of concurrent application of neuromodulation during task performance, especially when brief episodes of stimulation are used.

Previous studies on healthy human subjects have shown that anodal tDCS enhances cognition or motor learning [55–58] and these effects are specific to different levels of task difficulty [59, 60] or the site of tDCS [58, 61]. We found that anodal tDCS on M1 specifically enhanced the learning of the rotarod task, without affecting the learning of beam walking. Thus, even within the motor domain, concurrent tDCS can modulate specific motor functions. The mechanism underlying the task-specific tDCS effect was further

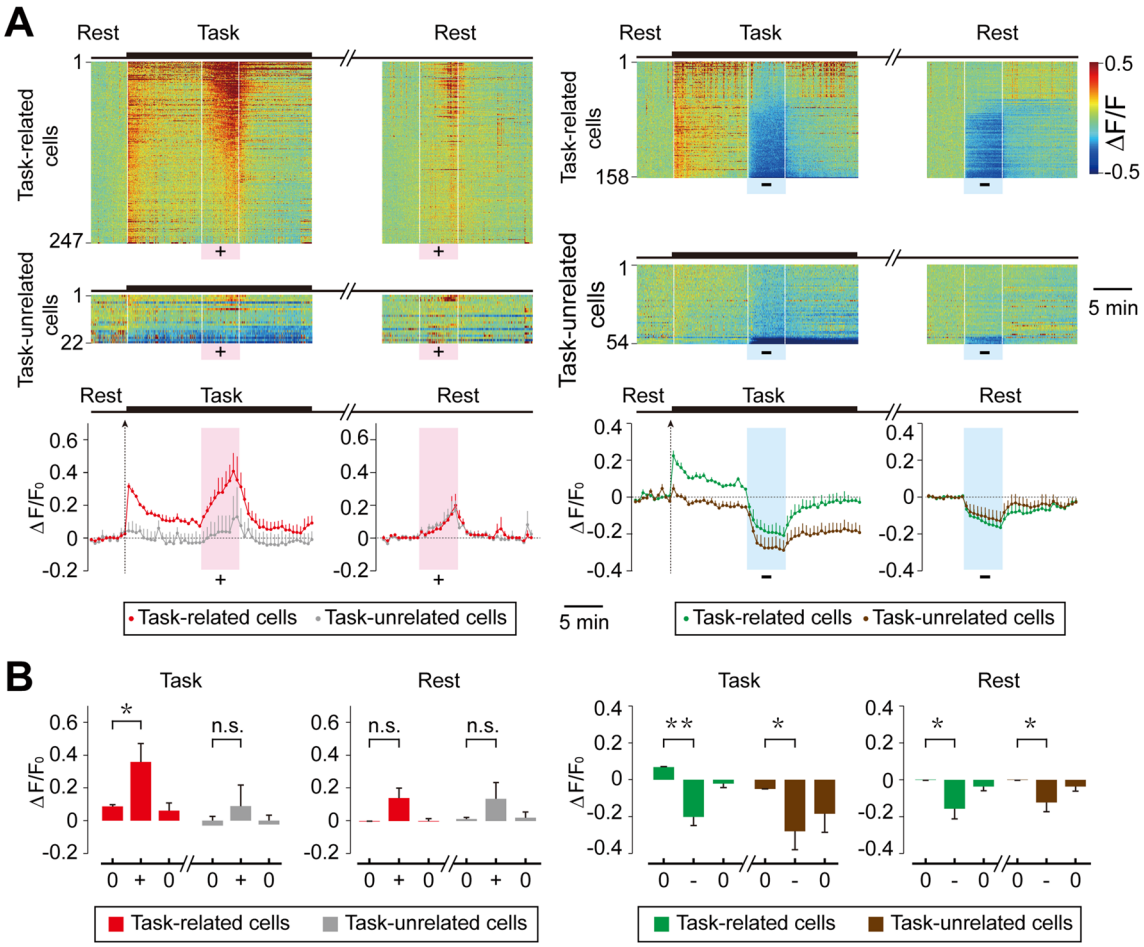

Fig. 4 Modulation of activity of task-related and task-unrelated cortical cells by tDCS. **A** Fluorescence changes ($\Delta F/F_0$) of task-related cells and task-unrelated cells within the imaged field (definitions in Methods) shown by activity heat maps of M1 cell populations. Upper panels, the amplitude of $\Delta F/F_0$ is normalized for each cell by the baseline during the 5-min period before the task onset and color-coded with the scale shown on the right. All cells (anodal: $n = 269$; cathodal: $n = 212$) recorded from 4 mice are grouped and ordered according to the peak values of $\Delta F/F_0$ within the tDCS time window. Lower panels, changes in the average $\Delta F/F_0$ with time during the experiment shown above for task-related and task-unrelated cells. Error bars, SEM. **B** Summary of tDCS-induced $\Delta F/F_0$ for data from all 4 mice. Average $\Delta F/F_0$ during the tDCS period ("+" or "-") were compared with those during the periods before and after tDCS ("0"). Histograms showing the average $\Delta F/F_0$ during the last 2 min of each period. Error bars, SEM; $^*P < 0.05$, $^{**}P < 0.01$, n.s. no significant difference, paired *t* test.

investigated in the present study using *in vivo* imaging of M1 neuronal activity. We showed that task-related M1 neurons were preferentially elevated by anodal tDCS, as compared to task-unrelated neurons, during the performance of the motor task. Thus, task-related circuit activation and potentiation account for the increase of motor functions induced by anodal tDCS. The same mechanism also accounts for the effect of low-frequency epidural alternating current stimulation (ACS) in improving grasping dexterity in macaque monkeys after lesion-induced stroke, where ACS has been shown to increase co-firing within task-related neural ensembles in the perilesional cortex [62]. Similarly, in chronic stroke patients, tDCS combined with locomotor training with a robotic gait orthosis improves motor restoration [63].

The tDCS current density used in the present study (3.2 mA/cm^2) was lower than that used by Pedron *et al.* [30] to study rat addictive behavior and working memory (5.7 mA/cm^2). This current density is 3–4 times lower than the upper limit of safe tDCS current determined in a rat study [64]. Cathodal tDCS at 5.7 mA/cm^2 has also been found to improve working memory and skill learning in rats [65]. Similar tDCS current levels have also been used in rats to treat status epilepticus (5.7 mA/cm^2) [66], to promote recovery from stoke-induced cognitive impairments (2.8 mA/cm^2) [67], and to elevate dopamine release in the striatum (3.2 mA/cm^2) [68]. In a previous *in vivo* Ca^{2+} imaging study on astrocyte activation by tDCS [25], the current density was 5.0 mA/cm^2, similar to the level used in our study. Notably,

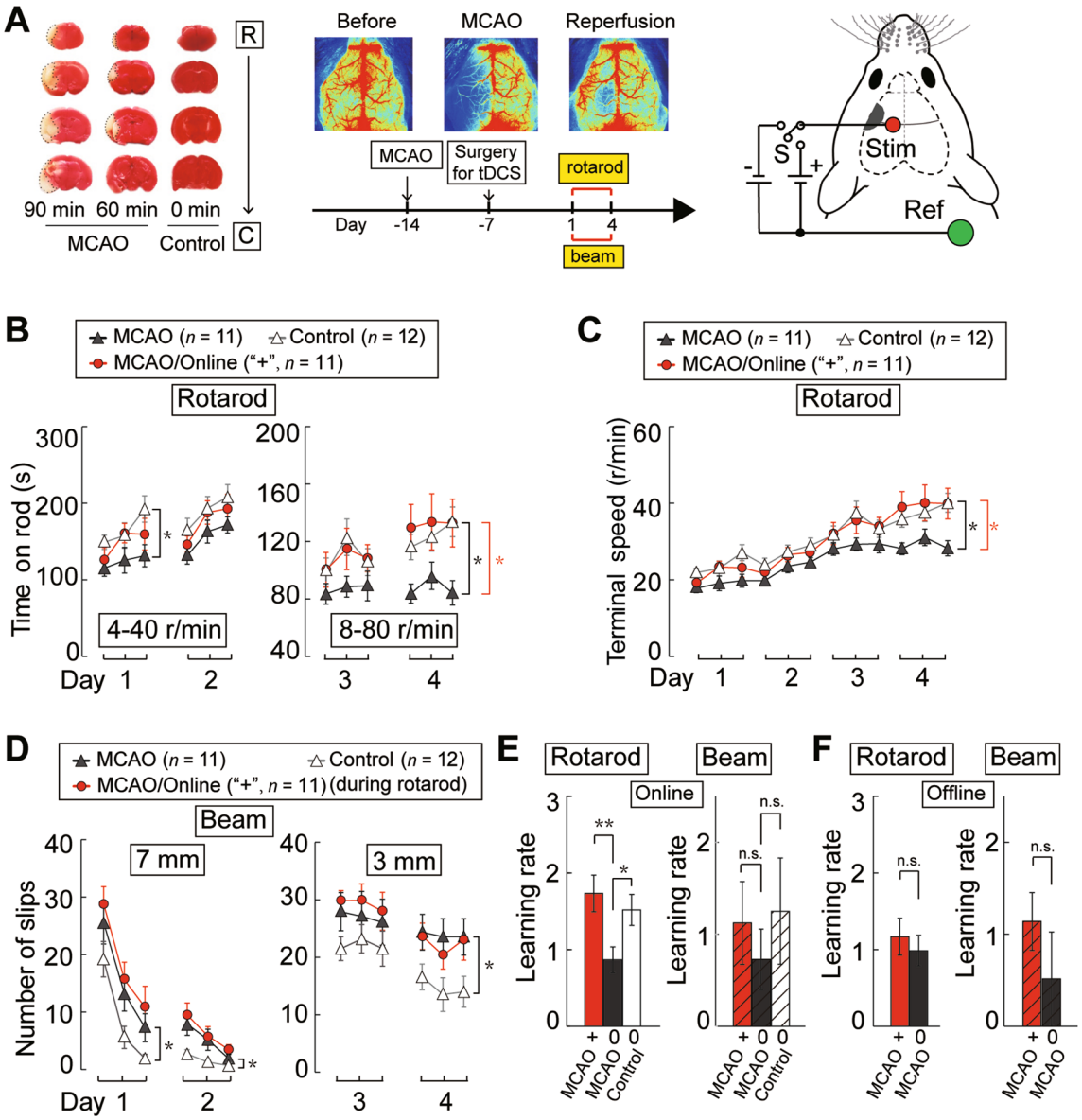

Fig. 5 Task-specific restoration of motor learning by online anodal tDCS in MCAO mice. **A** TTC staining (left) and laser speckle contrast imaging (upper middle) showing the lesion induced by MCAO that was maintained for 90, 60 or 0 min prior to reperfusion. Lower middle, time schedule of MCAO, surgery for tDCS, and training for rotarod running and beam walking. Right, schematic of placement of tDCS electrodes in MCAO mice. The infarct area is marked in gray, and the stimulating electrode ("Stim") covers parts of M1 and somatosensory cortex. **B**, **C** The average time on (**B**) and terminal speed (**C**) of the rotarod for MCAO mice with online anodal tDCS, sham stimulation, and sham MCAO surgery (control) in dual-task experiments, in which tDCS is applied only during rotarod running. Data are presented as in Fig. 1C and D. MCAO, mice subjected to 90-min occlusion of the MCA; Control (Sham-MCAO), mice subjected to the same surgery with no occlusion of the MCA; Online, MCAO mice with online tDCS during rotarod running; "*n*", total number of mice. **D** The average frequency of hindlimb slips (contralateral to the lesion) during beam walking. **E** Learning rates for rotarod running and beam walking in MCAO mice with online anodal tDCS. **F** Learning rates of rotarod and beam walking in MCAO mice with offline anodal tDCS. Offline, MCAO mice with tDCS before rotarod running; +, anodal tDCS; 0, no current. Error bars, SEM; $*P < 0.05$, $**P < 0.01$, n.s. no significant difference, two-way ANOVA in **B**–**D**, unpaired *t* test in **E**, **F**.

the standard current density applied to humans (0.029 and 0.057 mA/cm^2) [43, 69] is much lower than that used in rodent studies. This difference may be attributed to safety considerations, the effectiveness of current penetration through the skull and cortex, the electrode configuration, the extent of neuronal activity induced by the current, and the complexity of the neural networks.

The exact current density induced by tDCS in the cortex remains unclear. In our behavioral study, the effective current density of anodal tDCS was 3.2 mA/cm^2 at the surface

of the intact skull. Histological measurements of the thickness of the thinned skull of mice used in our Ca^{2+} imaging experiments yielded an average of 15.9 ± 0.86 μm (n = 4 mice). Thus, the average current density was estimated to be ~0.8 mA/cm^2 at the observation window (~2 mm in diameter) for the anodal current applied (25 μA), with a higher density near the center due to non-uniform current distribution. More precise estimation of the effective current density requires further analysis of the pattern of subdural currents, which depend on the electrode configuration and the resistance of various tissues.

We found that application of anodal tDCS to mouse M1 elevated cortical neuronal activity whereas cathodal tDCS suppressed it. These mechanisms could underlie the effects of tDCS on human motor cortex, where anodal tDCS increases and cathodal tDCS reduces corticospinal excitability (as revealed by TMS-induced MEP amplitudes) [22, 23, 70]. However, another study using cathodal tDCS of the human motor cortex showed a significant increase of corticospinal excitability at a total current of 2 mA and a decrease at 1 mA [71]. While the cause remains unclear, this finding underscores the importance of precise control of the magnitude of tDCS current. The tDCS acts by altering the neuronal membrane potential, and currents at different levels can activate or inhibit distinct populations of neurons that have different firing thresholds, leading to disparate functional effects.

In this study, task specificity was found in the enhancing effect of anodal tDCS on motor learning, but not in the suppressive effect of cathodal tDCS. This difference may result from our specific experimental paradigm, in which we used a 5-min ITI between sequential cathodal tDCS. Imaging experiments showed that this short interval did not allow complete recovery of neuronal activity following cathodal tDCS, thus producing offline inhibitory effect. By further adjustment of the ITI, it is possible that task-specific suppression could also be induced by cathodal tDCS.

Conclusions

In this study, we characterized the mechanism of action and an appropriate paradigm for the use of anodal tDCS in enhancing motor learning in normal mice and a mouse model of stroke. Our results suggest that concurrent application of anodal tDCS with the performance of a targeted task elevates the therapeutic efficacy. Our imaging results provide the neuronal mechanism underlying the effect of concurrent anodal tDCS in promoting task performance. This approach of concurrent neuromodulation could be applied to the treatment of other brain disorders, such as obsessive compulsive disorder, auditory hallucination in schizophrenia, epilepsy, and addiction. While the exact neural circuit abnormalities of many brain disorders remain to be identified, neuromodulation applied during voluntary or triggered disorder-associated behaviors could help to potentiate or suppress the underlying neural circuits, leading to therapeutic effects.

Acknowledgements We thank Drs. Yang Dan, Chun Xu, Liping Wang, Huatai Xu, and Zhiqi Xiong for suggestions; Dr. Huanhuan Zeng for technical support; and Dr. Zhijie Wang for providing the head-fixation holder and plates. This work was supported by the Strategic Priority Research Program of the Chinese Academy of Sciences (XDB32070100); the Shanghai Municipal Science and Technology Major Project (2018SHZDZX05); the Shanghai Key Basic Research Project (18JC1410100); Lingang Lab (LG202106-04-03 and LG202105-01-07); and the Shanghai Pilot Program for Basic Research – Chinese Academy of Science, Shanghai Branch (JCYJ-SHFY-2022-010).

Conflict of interest The authors declare no conflicts of interest.

References

1. Bestmann S, Walsh V. Transcranial electrical stimulation. Curr Biol 2017, 27: R1258–R1262.
2. Polanía R, Nitsche MA, Ruff CC. Studying and modifying brain function with non-invasive brain stimulation. Nat Neurosci 2018, 21: 174–187.
3. Kuo MF, Paulus W, Nitsche MA. Therapeutic effects of non-invasive brain stimulation with direct currents (tDCS) in neuropsychiatric diseases. Neuro Image 2014, 85(Pt 3): 948–960.
4. Gomez Palacio Schjetnan A, Faraji J, Metz GA, Tatsuno M, Luczak A. Transcranial direct current stimulation in stroke rehabilitation: A review of recent advancements. Stroke Res Treat 2013, 2013: 170256.
5. Fregni F, Boggio PS, Mansur CG, Wagner T, Ferreira MJL, Lima MC. Transcranial direct current stimulation of the unaffected hemisphere in stroke patients. Neuro Report 2005, 16: 1551–1555.
6. Hummel F, Celnik P, Giraux P, Floel A, Wu WH, Gerloff C, *et al*. Effects of non-invasive cortical stimulation on skilled motor function in chronic stroke. Brain 2005, 128: 490–499.
7. Yao J, Drogos J, Veltink F, Anderson C, Concha Urday Zaa J, Hanson LI, *et al*. The effect of transcranial direct current stimulation on the expression of the flexor synergy in the paretic arm in chronic stroke is dependent on shoulder abduction loading. Front Hum Neurosci 2015, 9: 262.
8. Hoy KE, Arnold SL, Emonson MRL, Daskalakis ZJ, Fitzgerald PB. An investigation into the effects of tDCS dose on cognitive performance over time in patients with schizophrenia. Schizophr Res 2014, 155: 96–100.
9. Brunoni AR, Zanao TA, Ferrucci R, Priori A, Valiengo L, de Oliveira JF, *et al*. Bifrontal tDCS prevents implicit learning acquisition in antidepressant-free patients with major depressive disorder. Prog Neuropsychopharmacol Biol Psychiatry 2013, 43: 146–150.
10. Oliveira JF, Zanão TA, Valiengo L, Lotufo PA, Benseñor IM, Fregni F, *et al*. Acute working memory improvement after tDCS in antidepressant-free patients with major depressive disorder. Neurosci Lett 2013, 537: 60–64.
11. Moezzi S, Ghoshuni M, Amiri M. Transcranial direct current stimulation (tDCS) effects on attention enhancement: A preliminary event related potential (ERP) study. Curr Psychol 2021: 1–7.

12. Gladwin TE, den Uyl TE, Fregni FF, Wiers RW. Enhancement of selective attention by tDCS: Interaction with interference in a Sternberg task. Neurosci Lett 2012, 512: 33–37.
13. Reteig LC, Newman LA, Ridderinkhof KR, Slagter HA. Effects of tDCS on the attentional blink revisited: A statistical evaluation of a replication attempt. PLoS One 2022, 17: e0262718.
14. Marangolo P, Fiori V, Calpagnano MA, Campana S, Razzano C, Caltagirone C, *et al*. tDCS over the left inferior frontal cortex improves speech production in aphasia. Front Hum Neurosci 2013, 7: 539.
15. You DS, Kim DY, Chun MH, Jung SE, Park SJ. Cathodal transcranial direct current stimulation of the right Wernicke's area improves comprehension in subacute stroke patients. Brain Lang 2011, 119: 1–5.
16. Fiori V, Cipollari S, Di Paola M, Razzano C, Caltagirone C, Marangolo P. tDCS stimulation segregates words in the brain: Evidence from aphasia. Front Hum Neurosci 2013, 7: 269.
17. Tanaka S, Takeda K, Otaka Y, Kita K, Osu R, Honda M, *et al*. Single session of transcranial direct current stimulation transiently increases knee extensor force in patients with hemiparetic stroke. Neurorehabil Neural Repair 2011, 25: 565–569.
18. Cha HK, Ji SG, Kim MK, Chang JS. Effect of transcranial direct current stimulation of function in patients with stroke. J Phys Ther Sci 2014, 26: 363–365.
19. Cruz Gonzalez P, Fong KNK, Chung RCK, Ting KH, Law LLF, Brown T. Can transcranial direct-current stimulation alone or combined with cognitive training be used as a clinical intervention to improve cognitive functioning in persons with mild cognitive impairment and dementia? A systematic review and meta-analysis. Front Hum Neurosci 2018, 12: 416.
20. Rahman A, Reato D, Arlotti M, Gasca F, Datta A, Parra LC, *et al*. Cellular effects of acute direct current stimulation: Somatic and synaptic terminal effects. J Physiol 2013, 591: 2563–2578.
21. Miranda PC, Lomarev M, Hallett M. Modeling the current distribution during transcranial direct current stimulation. Clin Neurophysiol 2006, 117: 1623–1629.
22. Nitsche MA, Paulus W. Sustained excitability elevations induced by transcranial DC motor cortex stimulation in humans. Neurology 2001, 57: 1899–1901.
23. Nitsche MA, Nitsche MS, Klein CC, Tergau F, Rothwell JC, Paulus W. Level of action of cathodal DC polarisation induced inhibition of the human motor cortex. Clin Neurophysiol 2003, 114: 600–604.
24. Fritsch B, Reis J, Martinowich K, Schambra HM, Ji Y, Cohen LG, *et al*. Direct Current stimulation promotes BDNF-dependent synaptic plasticity: Potential implications for motor learning. Neuron 2010, 66: 198–204.
25. Monai H, Hirase H. Astrocytic calcium activation in a mouse model of tDCS-Extended discussion. Neurogenesis (Austin) 2016, 3: e1240055.
26. de Vivo L, Melone M, Rothstein JD, Conti F. GLT-1 promoter activity in astrocytes and neurons of mouse *Hippocampus* and somatic sensory cortex. Front Neuroanat 2010, 3: 31.
27. Bolzoni F, Bączyk M, Jankowska E. Subcortical effects of transcranial direct current stimulation in the rat. J Physiol 2013, 591: 4027–4042.
28. Rahman A, Lafon B, Bikson M. Multilevel computational models for predicting the cellular effects of noninvasive brain stimulation. Prog Brain Res 2015, 222: 25–40.
29. Bikson M, Name A, Rahman A. Origins of specificity during tDCS: Anatomical, activity-selective, and input-bias mechanisms. Front Hum Neurosci 2013, 7: 688.
30. Pedron S, Monnin J, Haffen E, Sechter D, van Waes V. Repeated transcranial direct current stimulation prevents abnormal behaviors associated with abstinence from chronic nicotine consumption. Neuropsychopharmacology 2014, 39: 981–988.
31. Rothwell PE, Fuccillo MV, Maxeiner S, Hayton SJ, Gokce O, Lim BK, *et al*. Autism-associated neuroligin-3 mutations commonly impair striatal circuits to boost repetitive behaviors. Cell 2014, 158: 198–212.
32. Powell CM, Schoch S, Monteggia L, Barrot M, Matos MF, Feldmann N, *et al*. The presynaptic active zone protein RIM1α is critical for normal learning and memory. Neuron 2004, 42: 143–153.
33. Carter RJ, Lione LA, Humby T, Mangiarini L, Mahal A, Bates GP, *et al*. Characterization of progressive motor deficits in mice transgenic for the human Huntington's disease mutation. J Neurosci 1999, 19: 3248–3257.
34. Durukan A, Tatlisumak T. Acute ischemic stroke: Overview of major experimental rodent models, pathophysiology, and therapy of focal cerebral ischemia. Pharmacol Biochem Behav 2007, 87: 179–197.
35. Liu F, McCullough LD. Middle cerebral artery occlusion model in rodents: Methods and potential pitfalls. J Biomed Biotechnol 2011, 2011: 464701.
36. Murphy TH. Two-photon imaging of neuronal structural plasticity in mice during and after ischemia. Cold Spring Harb Protoc 2015, 2015: 548–557.
37. Li P, Murphy TH. Two-photon imaging during prolonged middle cerebral artery occlusion in mice reveals recovery of dendritic structure after reperfusion. J Neurosci 2008, 28: 11970–11979.
38. Armstead WM, Ganguly K, Kiessling JW, Riley J, Chen XH, Smith DH, *et al*. Signaling, delivery and age as emerging issues in the benefit/risk ratio outcome of tPA For treatment of CNS ischemic disorders. J Neurochem 2010, 113: 303–312.
39. Yang G, Chan PH, Chen J, Carlson E, Chen SF, Weinstein P, *et al*. Human copper-zinc superoxide dismutase transgenic mice are highly resistant to reperfusion injury after focal cerebral ischemia. Stroke 1994, 25: 165–170.
40. Bederson JB, Pitts LH, Germano SM, Nishimura MC, Davis RL, Bartkowski HM. Evaluation of 2, 3, 5-triphenyltetrazolium chloride as a stain for detection and quantification of experimental cerebral infarction in rats. Stroke 1986, 17: 1304–1308.
41. Miao P, Rege A, Li N, Thakor NV, Tong S. High resolution cerebral blood flow imaging by registered laser speckle contrast analysis. IEEE Trans Biomed Eng 2010, 57: 1152–1157.
42. Zhang QF, Li H, Chen M, Guo AK, Wen Y, Poo MM. Functional organization of intrinsic and feedback presynaptic inputs in the primary visual cortex. Proc Natl Acad Sci U S A 2018, 115: E5174–E5182.
43. Bennabi D, Pedron S, Haffen E, Monnin J, Peterschmitt Y, van Waes V. Transcranial direct current stimulation for memory enhancement: From clinical research to animal models. Front Syst Neurosci 2014, 8: 159.
44. Chen TW, Wardill TJ, Sun Y, Pulver SR, Renninger SL, Baohan A, *et al*. Ultrasensitive fluorescent proteins for imaging neuronal activity. Nature 2013, 499: 295–300.
45. Tada M, Takeuchi A, Hashizume M, Kitamura K, Kano M. A highly sensitive fluorescent indicator dye for calcium imaging of neural activity *in vitro* and *in vivo*. Eur J Neurosci 2014, 39: 1720–1728.
46. Medeiros LF, de Souza ICC, Vidor LP, de Souza A, Deitos A, Volz MS, *et al*. Neurobiological effects of transcranial direct current stimulation: A review. Front Psychiatry 2012, 3: 110.
47. Kronberg G, Bridi M, Abel T, Bikson M, Parra LC. Direct Current stimulation modulates LTP and LTD: Activity dependence and dendritic effects. Brain Stimul 2017, 10: 51–58.
48. Fregni F, El-Hagrassy MM, Pacheco-Barrios K, Carvalho S, Leite J, Simis M, *et al*. Evidence-based guidelines and secondary meta-analysis for the use of transcranial direct current stimulation in neurological and psychiatric disorders. Int J Neuropsychopharmacol 2020, 24: 256–313.

49. Bai X, Guo Z, He L, Ren L, McClure MA, Mu Q. Different therapeutic effects of transcranial direct current stimulation on upper and lower limb recovery of stroke patients with motor dysfunction: A meta-analysis. Neural Plast 2019, 2019: 1372138.
50. Nitsche MA, Schauenburg A, Lang N, Liebetanz D, Exner C, Paulus W, *et al*. Facilitation of implicit motor learning by weak transcranial direct current stimulation of the primary motor cortex in the human. J Cogn Neurosci 2003, 15: 619–626.
51. Stagg CJ, Jayaram G, Pastor D, Kincses ZT, Matthews PM, Johansen-Berg H. Polarity and timing-dependent effects of transcranial direct current stimulation in explicit motor learning. Neuropsychologia 2011, 49: 800–804.
52. Kidgell DJ, Goodwill AM, Frazer AK, Daly RM. Induction of cortical plasticity and improved motor performance following unilateral and bilateral transcranial direct current stimulation of the primary motor cortex. BMC Neurosci 2013, 14: 64.
53. Reis J, Schambra HM, Cohen LG, Buch ER, Fritsch B, Zarahn E, *et al*. Noninvasive cortical stimulation enhances motor skill acquisition over multiple days through an effect on consolidation. Proc Natl Acad Sci U S A 2009, 106: 1590–1595.
54. Ramanathan DS, Guo L, Gulati T, Davidson G, Hishinuma AK, Won SJ, *et al*. Low-frequency cortical activity is a neuromodulatory target that tracks recovery after stroke. Nat Med 2018, 24: 1257–1267.
55. Andrews SC, Hoy KE, Enticott PG, Daskalakis ZJ, Fitzgerald PB. Improving working memory: The effect of combining cognitive activity and anodal transcranial direct current stimulation to the left dorsolateral prefrontal cortex. Brain Stimul 2011, 4: 84–89.
56. Ohn SH, Park CI, Yoo WK, Ko MH, Choi KP, Kim GM, *et al*. Time-dependent effect of transcranial direct current stimulation on the enhancement of working memory. Neuroreport 2008, 19: 43–47.
57. Gill J, Shah-Basak PP, Hamilton R. It's the thought that counts: Examining the task-dependent effects of transcranial direct current stimulation on executive function. Brain Stimul 2015, 8: 253–259.
58. Saucedo Marquez CM, Zhang X, Swinnen SP, Meesen R, Wenderoth N. Task-specific effect of transcranial direct current stimulation on motor learning. Front Hum Neurosci 2013, 7: 333.
59. Pope PA, Brenton JW, Miall RC. Task-specific facilitation of cognition by anodal transcranial direct current stimulation of the prefrontal cortex. Cereb Cortex 2015, 25: 4551–4558.
60. Pope PA, Miall RC. Task-specific facilitation of cognition by cathodal transcranial direct current stimulation of the cerebellum. Brain Stimul 2012, 5: 84–94.
61. Karok S, Fletcher D, Witney AG. Task-specificity of unilateral anodal and dual-M1 tDCS effects on motor learning. Neuropsychologia 2017, 94: 84–95.
62. Khanna P, Totten D, Novik L, Roberts J, Morecraft RJ, Ganguly K. Low-frequency stimulation enhances ensemble co-firing and dexterity after stroke. Cell 2021, 184: 912-930.e20.
63. Danzl MM, Chelette KC, Lee K, Lykins D, Sawaki L. Brain stimulation paired with novel locomotor training with robotic gait orthosis in chronic stroke: A feasibility study. NeuroRehabilitation 2013, 33: 67–76.
64. Liebetanz D, Koch R, Mayenfels S, König F, Paulus W, Nitsche MA. Safety limits of cathodal transcranial direct current stimulation in rats. Clin Neurophysiol 2009, 120: 1161–1167.
65. Dockery CA, Liebetanz D, Birbaumer N, Malinowska M, Wesierska MJ. Cumulative benefits of frontal transcranial direct current stimulation on visuospatial working memory training and skill learning in rats. Neurobiol Learn Mem 2011, 96: 452–460.
66. Kamida T, Kong S, Eshima N, Abe T, Fujiki M, Kobayashi H. Transcranial direct current stimulation decreases convulsions and spatial memory deficits following pilocarpine-induced status epilepticus in immature rats. Behav Brain Res 2011, 217: 99–103.
67. Yoon KJ, Oh BM, Kim DY. Functional improvement and neuroplastic effects of anodal transcranial direct current stimulation (tDCS) delivered 1 day vs. 1 week after cerebral ischemia in rats. Brain Res 2012, 1452: 61–72.
68. Tanaka T, Takano Y, Tanaka S, Hironaka N, Kobayashi K, Hanakawa T, *et al*. Transcranial direct-current stimulation increases extracellular dopamine levels in the rat striatum. Front Syst Neurosci 2013, 7: 6.
69. Salehinejad MA, Wischnewski M, Ghanavati E, Mosayebi-Samani M, Kuo MF, Nitsche MA. Cognitive functions and underlying parameters of human brain physiology are associated with chronotype. Nat Commun 2021, 12: 4672.
70. Nitsche MA, Paulus W. Excitability changes induced in the human motor cortex by weak transcranial direct current stimulation. J Physiol 2000, 527: 633–639.
71. Batsikadze G, Moliadze V, Paulus W, Kuo MF, Nitsche MA. Partially non-linear stimulation intensity-dependent effects of direct current stimulation on motor cortex excitability in humans. J Physiol 2013, 591: 1987–2000.